Available online at www.sciencedirect.com

ScienceDirect

Procedia Engineering 105 (2015) 398 – 405

Procedia Engineering

www.elsevier.com/locate/procedia

6th BSME International Conference on Thermal Engineering (ICTE 2014)

MHD Convective Stagnation Flow of Nanofluid over a Shrinking Surface with Thermal Radiation, Heat Generation and Chemical Reaction

Mohammad Wahiduzzaman[a,*], Md. Shakhaoath Khan[b] and Ifsana Karim[b]

[a]*Mathematics Discipline, Science Engineering and Technology School,Khulna University, Khulna-9208, BANGLADESH*
[b]*Department of Chemical Engineering, School of Engineering, University of Newcastle, Callaghan, NSW 2308, AUSTRALIA.*

Abstract

The present study numerically investigates the phenomena of the steady two-dimensional magnetohydrodynamic(MHD) stagnation-point and heat-mass transfer flow of a nanofluid past a shrinking sheet with the influence of thermal radiation, heat generation and chemical reaction. The effect of Brownian motion and thermophoresis are well-thought-out instantaneously. A similarity solution is presented which depends on the magnetic parameter (M), Grashof number (G_r), modified Grashof number (G_m), heat generation parameter (Q), radiation parameter (R), Brownian motion number (N_b), thermophoresis number (N_t), Prandtl number (P_r), Lewis number (L_e), Chemical reaction parameter (γ) and the ratio of the rate constants of the shrinking velocity to the free stream velocity (α). A shooting technique is employed to solve this similarity model numerically. The results of the present analysis is going to observe the velocity, temperature, concentration, the wall shear stress, the Nusselt number and the Sherwood number at the different situation and dependency of different parameters. A comparative study is also being shown between the previously published results and the present results for the accuracy and interesting findings of the present research.

Peer-review under responsibility of organizing committee of the 6th BSME International Conference on Thermal Engineering (ICTE 2014)

Keywords: Magnetohydrodynamic stagnation-point flow, Heat transfer, Nanofluid, Shrinking sheet.

* Corresponding author. Mob.: + 880 1913 262715
E-mail address: wahidmathku@gmail.com

Peer-review under responsibility of organizing committee of the 6th BSME International Conference on Thermal Engineering (ICTE 2014)
doi:10.1016/j.proeng.2015.05.025

1. Introduction

Boundary layer flow behavior over a stretching surface is vital in engineering processes, such as, materials manufactured by extrusion, annealing and tinning of copper wires, glass blowing, continuous cooling and fibre spinning. At the time of manufacture of these sheets, the melt issues from a slit and is subsequently stretched to achieve the desired thickness and the final product of desired characteristic depends on the rate of cooling and the process of stretching. For the flow over a shrinking sheet, the fluid is attracted towards a slot and as a result it shows quite different characteristics from the stretching case. From a physical point of view, vorticity generated at the shrinking sheet is not confined within a boundary layer and a steady flow is not possible unless either a stagnation flow is applied or adequate suction is applied at the sheet. As discussed by Goldstein [1], this new type of shrinking flow is essentially a backward flow. Miklavcic and Wang [2] were the first who have investigated the flow over a shrinking sheet with suction effect. Steady two-dimensional and axisymmetric boundary layer stagnation point flow and heat transfer towards a shrinking sheet was analyzed by Wang [3]. The existence and uniqueness results for MHD stagnation point flow over a stretching/shrinking sheet were considered by Van Gorder et al.[4].. All studies mentioned above refer to the stagnation point flow towards a stretching/shrinking sheet in a viscous and Newtonian fluid. Bachok et al. [5] investigated the effects of solid volume fraction and the type of the nanoparticles on the fluid flow and heat transfer characteristics of a nanofluid over a shrinking sheet. Effects of magnetic field and thermal radiation on stagnation flow and heat transfer of nanofluid over a shrinking surface were investigated by Samir Kumar Nandy and Ioan Pop [6]. To the author's knowledge no studies have thus far been communicated with regard to MHD boundary layer stagnation flow and heat transfer of a nanofluid past a shrinking sheet with thermal radiation, heat generation and chemical reaction. The objective of the present work is therefore to extend the work of Samir Kumar Nandy and Ioan Pop [6] by taking Heat Generation and Chemical Reaction. The effects of magnetic field parameter (M), Brownian motion parameter (N_b), thermophoresis number (N_t), Prandtl number (P_r), Lewis number (L_e), radiation parameter (R), Grashof number (G_r), Modified Grashof umber (G_m), Chemical Reaction parameter (γ) and the velocity ratio parameter (α) on the relevant flow variables are described in detail. The present study is of immediate interest to all those processes which are highly affected with heat enhancement concept e.g. cooling of metallic sheets or electronic chips etc.

2. Flow analysis

Consider the steady two-dimensional MHD stagnation-point flow of an incompressible viscous electrically conducting nanofluid impinging normally on a shrinking sheet. The fluid is subjected to a uniform transverse magnetic field of strength B_0. Fig. 1 describes the physical model and the coordinate system, where the x and y axes are measured along the surface of the sheet and normal to it, respectively. It is assumed that the velocity of the stretching/shrinking sheet is $u_w(x) = cx$ and the velocity outside the boundary layer is $U(x) = ax$, where a and c are constants with $a > 0$. We note that $c > 0$ and $c < 0$ correspond to stretching and shrinking sheets respectively. Instantaneously at time $t > 0$, temperature of the plate and species concentration are raised to $T_w (> T_\infty)$ and $C_w (> C_\infty)$ respectively, which are thereafter maintained constant, where T_w, C_w are temperature and species concentration at the wall and T_∞, C_∞ are temperature and species concentration far away from the plate

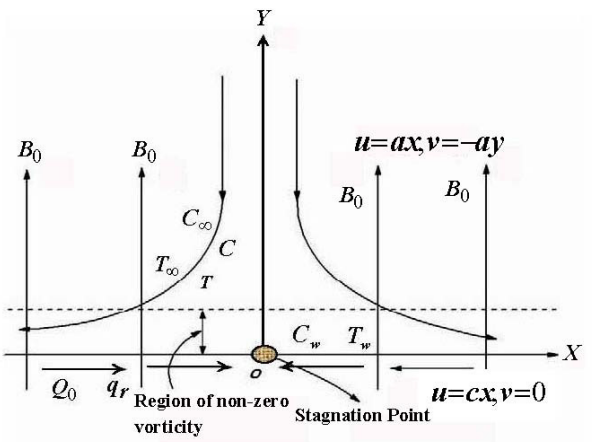

Fig.1. Physical model and coordinate system.

respectively.The basic steady conservation of mass, momentum, thermal energy and nanoparticles equations for nanofluids can be written in Cartesian coordinates x and y as,

$$\frac{\partial u}{\partial x}+\frac{\partial v}{\partial y}=0 \tag{1}$$

$$u\frac{\partial u}{\partial x}+v\frac{\partial u}{\partial y}=U\frac{du}{dx}+\upsilon\frac{\partial^2 u}{\partial y^2}+\frac{\sigma {B_0}^2}{\rho}(U-u)+g\beta(T-T_\infty)+g\beta^*(C-C_\infty) \tag{2}$$

$$u\frac{\partial T}{\partial x}+v\frac{\partial T}{\partial y}=\alpha_m\frac{\partial^2 T}{\partial y^2}-\frac{1}{\rho C_p}\frac{\partial q_r}{\partial y}+\tau\left[D_B\frac{\partial C}{\partial y}\frac{\partial T}{\partial y}+\frac{D_T}{T_\infty}\left(\frac{\partial T}{\partial y}\right)^2\right]+\frac{\overline{Q}}{\rho C_P}(T-T_w) \tag{3}$$

$$u\frac{\partial C}{\partial x}+v\frac{\partial C}{\partial y}=D_B\frac{\partial^2 C}{\partial y^2}+\frac{D_T}{T_\infty}\frac{\partial^2 T}{\partial y^2}-K_r(C-C_\infty) \tag{4}$$

In writing Eq. (2), we have neglected the induced magnetic field since the magnetic Reynolds number for the flow is assumed to be very small. This assumption is justified for flow of electrically conducting fluids such as liquid metals e.g., mercury, liquid sodium etc. Here u and v are the velocity components along the x and y directions, respectively, $U(x)$ is the free stream velocity, T is the fluid temperature and C is the nanoparticle volume fraction, σ is the electrical conductivity of the fluid, υ is the kinematic viscosity, α_m is the thermal diffusivity, ρ is the density of the base fluid, D_B is the Brownian diffusion coefficient, D_T is the thermophoresis diffusion coefficient, C_p is the specific heat at constant pressure, q_r is the radiative heat flux and τ is the ratio of the effective heat capacity of the nanoparticle material to the heat capacity of the ordinary fluid and K_r is the chemical reaction parameter. It is assumed that the wall temperature T_w and the nanoparticle volume fraction C_w are constant at the surface. Also when y tends to infinity, the ambient values of the temperature and the nanoparticle volume fraction attain to constant values of T_∞ and C_∞, respectively. The boundary conditions for the problem are;

$$\begin{aligned} &u=u_w=cx,\ v=0,\ T=T_w,\ C=C_w \quad \text{at} \quad y=0\\ &u\to U(x)=ax,\ \ T=T_\infty,\ C=C_\infty \qquad \text{as} \quad y\to\infty \end{aligned} \tag{5}$$

The radiative heat flux q_r is described by Rosseland approximation (see [35]) such that

$$q_r=-\frac{4\delta}{3k_1}\frac{\partial T^4}{\partial y} \tag{6}$$

where, δ is the Stefan-Boltzmann constant and K_1 is the mean absorption coefficient. Assuming the temperature difference with in the flow is such that T^4 can be expanded in a Taylor series about T_∞ and neglecting higher order terms, we get $T^4\approx 4{T_\infty}^3T-3{T_3}^4$. Hence from Eq. (6), using the above result, we have

$$\frac{\partial q_r}{\partial y}=-\frac{16\delta {T_\infty}^3}{3k_1}\frac{\partial^2 T}{\partial y^2} \tag{7}$$

2. Mathematical Formulation

To attain the similarity solution of Equations. (1)–(4) with the boundary conditions (Eq. (5)), the stream function and the dimensionless variables can be defined as follows:

$$\psi=x\sqrt{a\upsilon}\ f(\eta),\ \theta(\eta)=\frac{T-T_\infty}{T_w-T_\infty},\ \varphi(\eta)=\frac{C-C_\infty}{C_w-C_\infty},\ \eta=y\sqrt{\frac{a}{\upsilon}} \tag{8}$$

where the stream function ψ is defined in the usual way as $u = \frac{\partial \psi}{\partial y}$ and $v = -\frac{\partial \psi}{\partial x}$.

$\therefore u = axf'(\eta)$

$\therefore v = -\sqrt{a\upsilon}\, f(\eta)$

Using the above mentioned non-dimensional variable, the non-linear, non-dimensional, coupled ordinary differential equations have been obtained as;

$$f''' + ff'' - (f')^2 + M(1 - f') + \lambda_T \theta + \lambda_M \varphi = 0 \tag{9}$$

$$\frac{(1+4R)}{P_r}\theta'' + f\theta' + N_b\theta'\varphi' + N_t(\theta')^2 + Q\theta = 0 \tag{10}$$

$$\varphi'' + L_e\, f\, \varphi' + \frac{Nt}{Nb}\theta'' - \gamma\, R_e\, L_e\, \varphi = 0 \tag{11}$$

where the notation primes denote differentiation with respect to η and M is the dimensionless magnetic parameter, R is the thermal radiation parameter, G_r is the Grashof number, G_m is the Modified Grashof number, λ_T is the Thermal convective parameter, λ_M is the Mass convective parameter, P_r is the Prandtl number, and N_b is the Brownian motion parameter, N_t is the thermophoresis parameter, Q is the heat source parameter and L_e is the Lewis number, γ is the Chemical reaction parameter, R_e is the Local Reynolds number which are defined as

$$M = \frac{\sigma {B_0}^2}{\rho a}, G_r = \frac{g\beta x^3 (T_w - T_\infty)}{\upsilon^2}, G_m = \frac{g\beta^* x^3 (C_w - C_\infty)}{\upsilon^2}, \lambda_T = \frac{G_r}{{R_e}^2}, \lambda_M = \frac{G_m}{{R_e}^2} P_r = \frac{\upsilon}{\alpha_m}, R = \frac{4\delta {T_\infty}^3}{3k_1\alpha_m \rho C_p},$$

$$Q = \frac{\overline{Q}}{\rho C_p a} N_b = \frac{\tau D_B (C_w - C_\infty)}{\upsilon}, N_t = \frac{\tau D_T (T_w - T_\infty)}{\upsilon T_\infty}, L_e = \frac{\upsilon}{D_B}, \gamma = \frac{K_r \upsilon}{U^2} \text{ and } R_e = \frac{U x}{\upsilon} \tag{12}$$

Eq. (10) shows that the temperature actually does not depend on Prandtl number (P_r) and the thermal radiation parameter (R) independently, but depends only on a combination of them which is the effective Prandtl number (P_{reff}). Introducing the effective Prandtl number $P_{reff} = \frac{P_r}{1+4R}$, Eq.(10) can be written as

$$\frac{1}{P_{reff}}\theta'' + f\theta' + N_b\theta'\varphi' + N_t(\theta')^2 + Q\theta = 0 \tag{13}$$

The effect of the thermal radiation in the linearized Rosseland approximation on the heat transfer characteristics of various boundary layer flows is discussed in some details in the reference [36].

The corresponding boundary conditions are

$$\begin{aligned} &f(0) = 0,\ f'(0) = \alpha = \frac{c}{a},\ \theta(0) = 1,\ \varphi(0) = 1 && \text{at} \quad \eta = 0 \\ &f'(\eta) \to 1,\ \theta(\eta) \to 0,\ \varphi(\eta) \to 0 && \text{as} \quad \eta \to \infty \end{aligned} \tag{14}$$

where α is the ratio of the rates of the stretching/shrinking velocity and the free stream velocity.

It is to be noted that this boundary value problem reduces the classical problem of flow and heat transfer due to a stretching/shrinking surface in a viscous fluid when $N_b = N_t = 0$. In this case, the boundary value problem for φ becomes ill-posed without physical significance. The physical quantities of interest are the skin friction coefficient C_f, the local Nusselt number Nu_x and the local Sherwood number Sh_x which are defined as

$$C_f = \frac{\tau_w}{\rho U^2(x)}, Nu_x = \frac{x q_w}{k(T_w - T_\infty)}, Sh_x = \frac{x q_m}{D_B (C_w - C_\infty)} \tag{15}$$

where τ_w is the shear stress along the stretching surface, q_w and q_m are the wall heat and mass fluxes, respectively. Hence, using Eqs. (8) and (15), we get

$$R_{e_x}^{\frac{1}{2}} C_f = f''(0)\,,\ Nu_x R_{e_x}^{-\frac{1}{2}} = -\theta'(0)\,,\ Sh_x R_{e_x}^{-\frac{1}{2}} = -\varphi'(0) \tag{16}$$

where, $R_{e_x} = \dfrac{U(x)x}{\upsilon}$ is the local Reynolds number based on the free stream velocity $U(x)$.

3. Results and discussion

Equations. (9), (11) and (13) subject to the boundary conditions (Eq. (14)) have been solved numerically using sixth order Rung–Kutta method with shooting technique for some values of the physical parameters involved in the present problem. In order to investigate the physical representation of the problem, the numerical values of velocity (f') temperature (θ) and concentration (φ) have been computed for resultant principal parameters. Fig. 2 shows the trajectories of skin friction coefficient $f''(0)$ with $\alpha < 0$ (shrinking sheet) and $\alpha > 0$ (stretching sheet) for

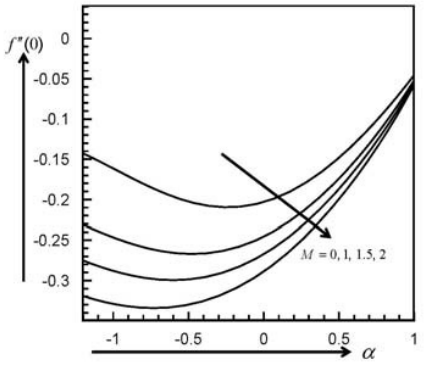

Fig. 2. Variation of the skin friction coefficient $f''(0)$ with α for different values of the magnetic parameter M with $N_b = N_t = 0.1$, $L_e = 2$, $P_r = 5$, $\lambda_1 = 2$, $\lambda_{1b} = 2$, $\gamma = 1$, $R_e = 1$ and $R = 0.5$.

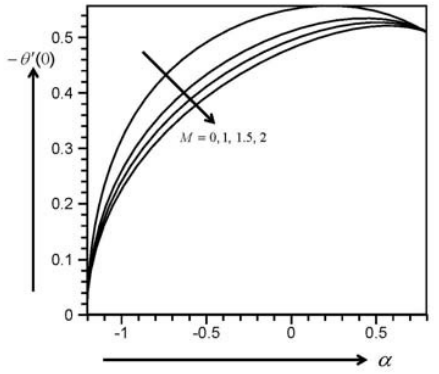

Fig. 3. Variation of the Nusselt number $-\theta'(0)$ with α for different values of the magnetic parameter M with $N_b = N_t = 0.1$, $L_e = 2$, $P_r = 5$, $\lambda_1 = 2$, $\lambda_{1b} = 2$, $\gamma = 1$, $R_e = 1$ and $R = 0.5$.

different values of the magnetic parameter (M). The figure reveals that the values of $f''(0)$ decreases as $|\alpha|$ decreases In Fig. 3, the temperature gradient at the sheet (the Nusselt number) $-\theta'(0)$, which is proportional to the rate of heat transfer from the sheet, is plotted for different values of the magnetic parameter M. It is observed that $|-\theta'(0)|$ decreases with an increase in M. On the other hand, influence of the magnetic parameter M on the Sherwood number $-\varphi'(0)$ is shown in Fig. 4. The figure reveals that $|-\varphi'(0)|$ decreases when M increases.

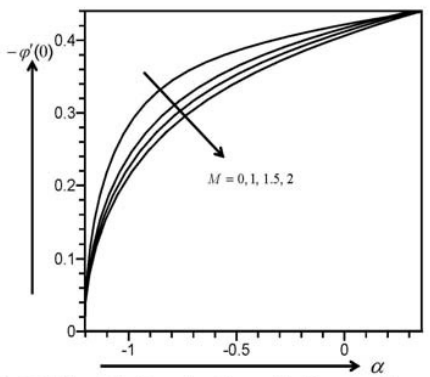

Fig. 4. Variation of the Sherwood number $-\varphi'(0)$ with α for different values of the magnetic parameter M with $N_b = N_t = 0.1$, $L_e = 2$, $P_r = 5$, $\lambda_1 = 2$, $\lambda_{1b} = 2$, $\gamma = 1$, $R_e = 1$ and $R = 0.5$.

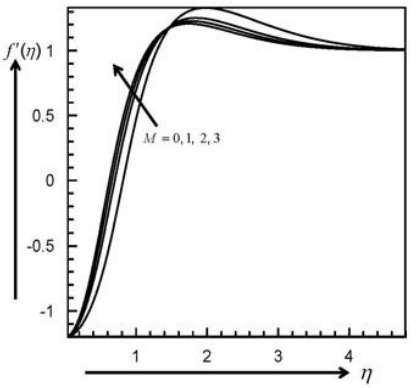

Fig.5. Variation of the velocity profiles $f'(\eta)$ for several values of M with $\alpha = -1.20$ $N_b = N_t = 0.1$, $L_e = 1$, $P_r = 1$, $\lambda_1 = 2$, $\lambda_{1b} = 2$, $\gamma = 1$, $R_e = 1$ and $R = 0.2$.

The effect of the magnetic parameter (M) on the horizontal velocity component $f'(\eta)$ is shown in Fig. 5. The figure indicates that the velocity increases with the increasing values of the magnetic parameter (M). From a physical point of view, this follows from the fact that as in this case, Lorentz force is positive and consequently as M increases, this Lorentz force is also increases and hence accelerates the flow. Fig. 6 represents the variation of the temperature distribution $\theta(\eta)$ for several values of M. The figure exhibits the temperature decreases with increase in M. Physically this is explained as follows. The extent of reverse cellular flow above the sheet decreases with increase in M and as a result, the temperature field is influenced by the advection of the fluid velocity above the sheet. The effects of the Brownian motion parameter (N_b) and thermophoresis parameter (N_t) on temperature profiles $\theta(\eta)$ are shown in Figs. 7 and 8. It is observed that with the increasing values of N_b and N_t, the fluid temperature decreases and increases respectively. For small particles, Brownian motion is strong and the parameter N_b will have high values and for large particles, N_b will have small values. Hence Brownian motion can exert a significant enhancing influence on temperature profiles and the temperature in the boundary layer increases with the increase in N_b. Again thermophoresis parameter (N_t) also serves to warm the boundary layer for low values of Prandtl number (P_r) and Lewis number (L_e). Fig. 9 shows the influence of effective Prandtl number (P_{reff}) on the temperature profile $\theta(\eta)$ for fixed values of other parameters. It is to be noted that P_{reff} is nothing but a simple rescaling of the Prandtl number (P_r) by a factor

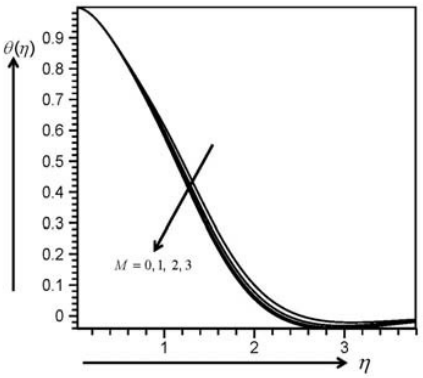

Fig.6. Variation of the temperature profiles $\theta(\eta)$ for several values of M with $\alpha = -1.20$ $N_b = N_t = 0.1$, $L_e = 1$, $P_r = 1$, $\lambda_1 = 2$, $\lambda_{1e} = 2$, $\gamma = 1$, $R_e = 1$ and $R = 0.2$.

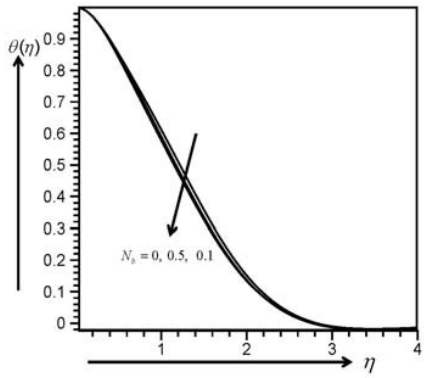

Fig.7. Variation of the temperature profiles $\theta(\eta)$ for several values of N_b with $\alpha = -1.20$ $N_t = 0.1$, $L_e = 1$, $M = 0.1$, $P_r = 0.71$, $\lambda_1 = 2$, $\lambda_{1e} = 2$, $\gamma = 1$, $R_e = 1$ and $R = 0.2$.

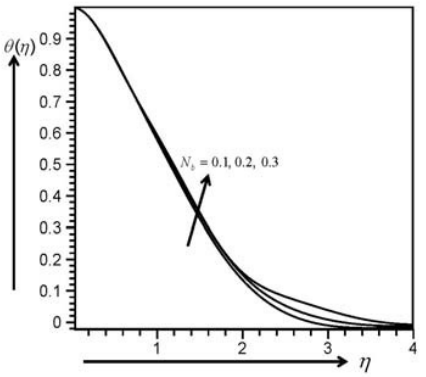

Fig.8. Variation of the temperature profiles $\theta(\eta)$ for several values of N_b with $\alpha = -1.20$ $N_t = 0.1$, $L_e = 1$, $M = 0.1$, $P_r = 0.71$, $\lambda_1 = 2$, $\lambda_{1e} = 2$, $\gamma = 1$, $R_e = 1$ and $R = 0.2$.

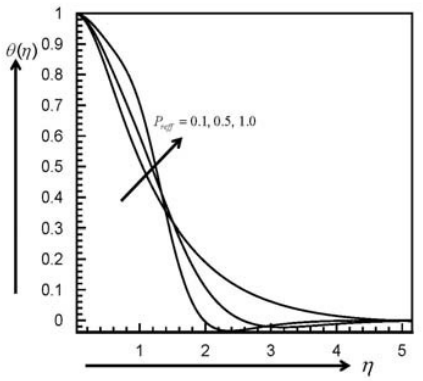

Fig.9. Variation of the temperature profiles $\theta(\eta)$ for several values of P_{reff} with $\alpha = -1.20$ $N_b = N_t = 0.1$, $L_e = 1$, $M = 0.1$, $\lambda_1 = 2$, $\lambda_{1e} = 2$, $\gamma = 1$, $R_e = 1$ and $R = 0.2$.

involving the radiation parameter (R). It is observed from the figure that the temperature at a point decreases with an increase in the effective Prandtl number except a small region near the sheet for the first solution branch. From a physical point of view, if P_{reff} increases, the thermal diffusivity decreases and this phenomenon leads to decrease the thermal boundary layer thickness. But, interestingly, for the second solution, up to a certain region, $\theta(\eta)$ increases as P_{reff} increases and beyond this region, $\theta(\eta)$ decreases as P_{reff} increases. The variation of the concentration profiles $\varphi(\eta)$ for different values of the Lewis number (L_e) and Brownian motion parameter (N_b) are shown in Figs. 10 and 11, respectively. Generally Lewis number, the ratio of thermal diffusivity to mass diffusivity, is used to characterize fluid flows where there is simultaneous heat and mass transfer by convection. Fig. 10 shows that the solution branches of $\varphi(\eta)$ decreases with an increase in L_e. The same feature as in the case of L_e is also observed for the Brownian motion parameter N_b and is depicted in Fig. 11. Presentation of full stability

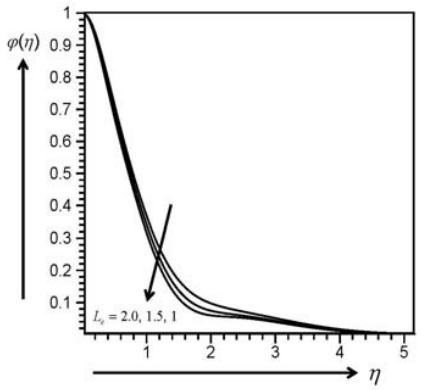

Fig.10. Variation of the concentration profiles $\varphi(\eta)$ for several values of L_e with $\alpha = -1.20$ $N_b = N_t = 0.1$, $M = 0.1$, $P_r = 0.71$, $\lambda_1 = 2$, $\lambda_{01} = 2$, $\gamma = 1$, $R_e = 1$ and $R = 0.2$.

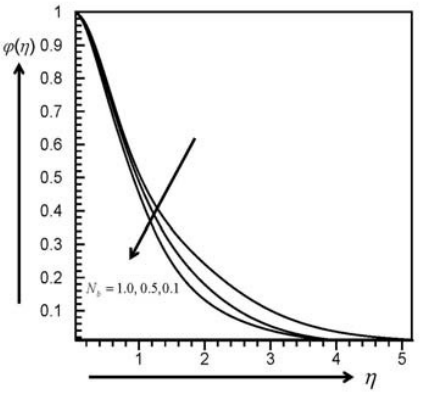

Fig.11. Variation of the concentration profiles $\varphi(\eta)$ for several values of N_b with $\alpha = -1.20$ $N_t = 0.1$, $L_e = 1.0$ $M = 0.1$, $P_r = 0.71$, $\lambda_1 = 2$, $\lambda_{01} = 2$, $\gamma = 1$, $R_e = 1$ and $R = 0.2$

analysis is beyond the scope of the present work since a stability analysis requires an unsteady flow, whereas our problem is a steady one.

3. Conclusion

The present paper deals with the analysis of MHD Convective Stagnation Flow of Nanofluid over a Shrinking Surface in the presence of thermal radiation, heat generation and chemical reaction. Numerical solutions of the resulting system of nonlinear ordinary differential equations are obtained by using the shootingmethod coupled with Runge-Kutta scheme. The effects of various parameters such as magnetic field parameter (M), Brownian motion parameter (N_b), thermophoresis number (N_t), Prandtl number (P_r), Lewis number (L_e), radiation parameter (R), Grashof number (G_r), Modified Grashof umber (G_m), Chemical Reaction parameter (γ) and the velocity ratio parameter (α) on the dimensionless velocity, temperature, and concentration profiles have been studied graphically. The influence of different parameters of on the skin friction, Nusselt number, and Sherwood number are shown graphically as well. From the present numerical investigation, the following inferences can be drawn:

- **i.** Velocity increases but temperature profile decreases with the increasing values of M.
- **ii.** With the increasing values of N_b and N_t, the fluid temperature decreases and increases respectively.
- **iii.** It is observed that the temperature at a point decreases with an increase in the effective Prandtl number.
- **iv.** The solution branches of $\varphi(\eta)$ decreases with an increase in L_e. The same feature as in the case of L_e is also observed for the Brownian motion parameter N_b.

Acknowledgment

We thank the reviewer for his useful comments and suggestions that led to definite improvement in the paper.

References

[1] S. Goldstein, On backward boundary layers and flow in converging passages, J. Fluid Mech. 21 (1965) 33–45.
[2] M. Miklavcic, C.Y. Wang, Viscous flow due to a shrinking sheet, Q. Appl. Math. 64(2006) 283–290.
[3] C.Y. Wang, Stagnation flow towards a shrinking sheet, Int. J. Nonlinear Mech. 43(2008) 377–382.
[4] R.A. Van Gorder, K. Vajravelu, I. Pop, Hydromagnetic stagnation-point flow of a viscous fluid over a stretching/shrinking sheet, Meccanica 47 (1) (2012) 31–50.
[5] N. Bachok, A. Ishak, I. Pop, Stagnation-point flow over a stretching/shrinking sheet in a nanofluid, Nanoscale Res. Lett. 6 (2011) 623–632.
[6] Samir Kumar Nandy, Ioan Pop, Effects of magnetic field and thermal radiation on stagnation flow and heat transfer of nanofluid over a shrinking surface, . International Communications in Heat and Mass Transfer 53 (2014) 50–55.